

- Rigo, A., Viglino, P., Rotilio, G., & Tomat, R. (1975) *FEBS Lett.* 50, 86-88.
- Rigo, A., Stevanato, R., Viglino, P., & Rotilio, G. (1977) *Biochem. Biophys. Res. Commun.* 79, 776-783.
- Rigo, A., Viglino, P., Bonori, M., Cocco, D., Calabrese, L., & Rotilio, G. (1978) *Biochem. J.* 169, 277-280.
- Rigo, A., Viglino, P., Argese, E., Terenzi, M., & Rotilio, G. (1979) *J. Biol. Chem.* 254, 1759-1760.
- Rotilio, G., Finazzi-Agrò, A., Calabrese, L., Bossa, F., Guerrieri, P., & Mondovì, B. (1971) *Biochemistry* 10, 616-621.
- Rotilio, G., Rigo, A., & Calabrese, L. (1978) in *Frontiers in Physicochemical Biology*, pp 357-368, Academic, New York.
- Terenzi, M., Rigo, A., Franconi, C., Mondovì, B., Calabrese, L., & Rotilio, G. (1974) *Biochim. Biophys. Acta* 351, 230-236.
- Viglino, P., Rigo, A., Stevanato, R., Ranieri, G., Rotilio, G., & Calabrese, L. (1979) *J. Magn. Reson.* 34, 265-274.
- Viglino, P., Rigo, A., Argese, E., Calabrese, L., Cocco, D., & Rotilio, G. (1981) *Biochim. Biophys. Res. Commun.* 100, 125-130.

Isolation and Characterization of a New Zinc-Binding Protein from Albacore Tuna Plasma[†]

Bruce Dyke, Jack Hegenauer, and Paul Saltman*

Department of Biology, University of California, San Diego, La Jolla, California 92093

R. Michael Laurs

Southwest Fisheries Center, National Oceanic and Atmospheric Administration, U.S. Department of Commerce, La Jolla, California 92037

Received July 18, 1986; Revised Manuscript Received January 29, 1987

ABSTRACT: The protein responsible for sequestering high levels of zinc in the plasma of the albacore tuna (*Thunnus alalunga*) has been isolated by sequential chromatography. The glycoprotein has a molecular weight of 66 000. Approximately 8.2% of its amino acid residues are histidines. Equilibrium dialysis experiments show it to bind 3 mol of zinc/mol of protein. The stoichiometric constant for the association of zinc with a binding site containing three histidines was determined to be $10^{9.4}$. This protein is different from albumin and represents a previously uncharacterized zinc transport protein.

High levels of zinc, relative to other trace elements, in the tissue of fish have been recognized for a long time (Vinogradov, 1953). Plasma of the albacore tuna (*Thunnus alalunga*), for example, has a zinc level more than 12 times higher than human serum. It is clear from the work of many investigators [see Vallee (1959)] that in biological systems zinc must exist as complexes with organic ligands rather than as free ions in solution. This paper presents our isolation and investigation of the plasma protein in albacore which is responsible for complexing the large amount of endogenous zinc. Fletcher and Fletcher (1978) described a similar Zn-binding protein(s) in winter flounder responsible for binding almost all plasma zinc.

Since zinc in plasma is chelated to endogenous ligands, only high-affinity sites on a plasma-binding protein are likely to be occupied under biological conditions. We have therefore designed experiments to characterize such sites by chelating the zinc with a well-characterized ligand in order to prevent hydrolysis and to form a mathematical basis with which to quantitate the competition for protein uptake of this metal. Experiments using competitive chelation to modulate zinc binding to proteins have been carried out with some enzymes (Cohen & Wilson, 1966; Billo et al., 1978). We have generalized this approach to multicomponent zinc-binding systems and have adapted the traditional Scatchard analysis of equilibrium binding to investigate the high-affinity Zn-binding sites on the tuna protein.

MATERIALS AND METHODS

Albacore Plasma. Albacore were captured with hook-and-line in the Pacific Ocean within 200 miles of San Diego during the months of July and August of 1979-1983 aboard the N.O.A.A. research vessel *David Starr Jordan*. Blood was collected immediately in syringes by cardiac puncture. Because blood clotting and clot dissolution occur almost simultaneously in this fish, true "serum" was not obtained; rather, plasma was collected within 30 min of bleeding after centrifugation of red cells at approximately 2000g for 15 min at room temperature. Plasma was stored frozen at -18°C .

Radiozinc Solutions. $^{65}\text{ZnCl}_2$ ("carrier-free"; New England Nuclear Corp., Boston, MA; specific activity 6-7 mCi/mg) was diluted into 0.1 N HCl prior to use. Radioactivity measurements were made in a Nuclear-Chicago Model 1085 γ well counter with the spectrometer calibrated to capture the 1.11-MeV emission ($\pm 10\%$) of ^{65}Zn .

Protein Purification. (A) *Rationale for Purification.* At the beginning of our studies, we were able only to distinguish the tuna plasma Zn-binding protein as one of the two most anodal "albumin-like" bands in sodium dodecyl sulfate (SDS) gel electrophoresis (data not shown). For purification, we therefore explored chromatographic systems that would fractionate these two bands, which seemed similar in size and electrophoretic mobility, on the basis of properties other than charge alone. Metal-chelating resins with iminodiacetate functionalities have been used successfully for affinity chromatography of other metal-binding proteins (Muszynska et al., 1986). Lectin affinity chromatography has been of value in the separation of various non-glycoprotein plasma albumins

[†] This work was supported by USPHS Grant AM-12386.

* Correspondence should be addressed to this author.

(Hrkal & Vodrazka, 1977; Aspberg & Porath, 1970). After performing numerous development studies, we adopted a three-step chromatographic procedure that yielded a purified fraction showing a single band on SDS gel electrophoresis.

The Zn-binding protein of plasma was purified as described below by sequential chromatography on (a) Sepharose 6B (Pharmacia) reduced with borohydride according to Lonnerdal and Hoffman (1981), (b) chelating Sepharose 6B, and (c) concanavalin A-Sepharose 4B. All columns were run at room temperature. In order to facilitate tracing of the Zn-binding components, plasma was labeled with $^{65}\text{ZnCl}_2$ by adding a small quantity of "carrier-free" $^{65}\text{ZnCl}_2$ to give approximately 6×10^4 cpm/mL of plasma.

(B) Gel Filtration Chromatography. One milliliter of labeled plasma was dialyzed against equilibration buffer [0.01 M *N*-(2-hydroxyethyl)piperazine-*N'*-2-ethanesulfonic acid (HEPES), 1.0 M NaCl, and 0.02% phenylmethanesulfonyl fluoride (PMSF), pH 7.0] and applied to a 1.5×51.5 cm column of Sepharose 6B. The radioactive peak was pooled. Figure 1 shows a typical elution profile.

(C) Zinc Affinity Chromatography. A column of chelating Sepharose 6B (1.0×28.5 cm) was prepared by applying 50 mL of 22 mM ZnSO_4 to saturate the iminodiacetic acid residues. The column was subsequently washed with equilibration buffer (0.01 M HEPES, 1.0 M NaCl, and 0.02% PMSF, pH 7.0) to remove unbound zinc. The pooled radioactive protein peak from the preceding step was then applied. The column was rinsed with 1 column volume of buffer to remove unbound protein. Bound protein was removed with a linear gradient of decreasing pH formed by continuous mixing (Hegenauer et al., 1965) of 30 mL of 0.01 M sodium acetate (NaOAc) and 0.02% PMSF, pH 5.0, with 30 mL of 0.01 M NaOAc and 0.02% PMSF, pH 2.0 (HCl). Figure 2 shows a typical elution profile. Radioactive zinc was lost from the protein in the pH gradient; therefore, all protein peaks were checked for zinc uptake by using equilibrium dialysis in order to identify the zinc-binding peak(s). Zn binding was found only in the last peak from the gradient. The last protein peak was eluted at pH 3.0 during protonation of the iminodiacetic acid residues, causing ionic zinc to be released into solution. The protein peak was pooled, but before the protein solution was neutralized, excess ionic zinc was removed by repeated ultrafiltration through an Amicon Model 8010 stirred ultrafiltration cell (10000 molecular weight cutoff membrane) using pH 3.0 NaOAc washes. The pH was increased to 7.0 by dialysis against the subsequent column buffer.

(D) Lectin Affinity Chromatography. The Zn-binding peak was then applied to concanavalin A-Sepharose 4B (1×17 cm). Approximately 2 column volumes of equilibration buffer (0.02 M NaH_2PO_4 , 1.0 M NaCl, and 0.02% PMSF, pH 7.0) were applied to remove all unbound proteins. Bound proteins were eluted with 0.5 M methyl mannoside dissolved in equilibration buffer. One-half column volume of elution buffer was applied to the column and then allowed to stand and equilibrate for 30 min. Elution was continued for approximately 2 column volumes. The column was then washed with the starting buffer, and protein peaks were collected. Figure 3 shows a typical elution profile.

(E) Removal of Metal. Several batches of protein were purified as described above, checked for electrophoretic purity, and pooled. The protein was rendered zinc free by adjusting the pH to 3.0 with HCl and repeatedly washing it on an ultrafiltration membrane with 10-mL portions of 10 mM sodium acetate/HCl, pH 3.0, until the ultrafiltrate contained less than 50 nM zinc. Stock protein solution was finally

equilibrated by dialysis with the same buffer and electrolyte system used in subsequent experiments. The zinc content of this protein solution was determined by graphite furnace atomic absorption spectrophotometry to be 34 nM. This "background" level of zinc had no significant effect on our results. Protein concentration was determined by the method of Lowry et al. (1951) using a bovine serum albumin standard.

Electrophoresis. Electrophoresis was carried out in an 8% polyacrylamide slab gel prepared with final concentrations of 0.375 M tris(hydroxymethyl)aminomethane hydrochloride (Tris-HCl)/0.1% sodium dodecyl sulfate (SDS), pH 8.8, with a 3% stacking gel. The ratio of acrylamide:bis(acrylamide) was 29.1:0.9. Ten microliters of *N,N,N',N'*-tetramethylethylenediamine (TEMED) per 20-mL total volume and 0.03% ammonium persulfate were used to catalyze polymerization. Running buffer was 0.025 M Tris-glycine/0.4% SDS, pH 8.9. All gels were run at 45-mA constant current for approximately 2.5 h, using the gel apparatus described by Studier (1973). Bio-Rad SDS-polyacrylamide gel electrophoresis (PAGE) low molecular weight standards were used as markers. Gels were stained by using the Kodavue electrophoresis visualization kit (Eastman Kodak). The concentration of applied protein was determined by the method of Lowry et al. (1951).

Amino Acid Analysis. Protein was hydrolyzed in 6 N HCl for 24 h at 110 °C in sealed evacuated tubes. Analysis was performed by using a Beckman 118C analyzer.

Zinc Chelates. Stock solutions of reagent-grade $\text{ZnSO}_4 \cdot 6\text{H}_2\text{O}$, HEPES, NaCl, and disodium nitrilotriacetate (NTA) were prepared in quartz-distilled water. In preparation of the radiozinc chelate for dialysis experiments, $^{65}\text{ZnCl}_2$ was equilibrated with zinc sulfate for 15 min; the total zinc concentration from $^{65,38}\text{Zn}$ plus ^{65}Zn was calculated by reference to radiochemical specifications before addition of NTA. The NTA:Zn molar ratio was 1.1:1. The final specific activity of the zinc chelate was 0.348 mCi/mg. Radiozinc was at most 5% of the total zinc. HEPES and NaCl were added to final concentrations of 0.03 and 0.25 M, respectively. A small amount of dilute 0.01 N NaOH was added to achieve the final pH before diluting to volume. Ligand concentration was calculated from the concentration of stock solutions.

Equilibrium Dialysis. Experiments were performed in plastic cell compartments separated by a single thickness of no. 20 Visking tubing (Union Carbide Corp.) as described by Malmstrom (1953); the interior of the cells was coated lightly with silicone grease to prevent adsorption of zinc to the acrylic surface. One milliliter of protein solution and 1.0 mL of radiozinc chelate were pipetted on opposite sides of the membrane. Filling holes were sealed with tape, and cells were agitated on a reciprocal shaker (~ 1 excursion/sc) for 3 days at 4 ± 0.5 °C. Samples (850 μL) were withdrawn from each cell compartment for measurement of ^{65}Zn . The proportion of protein-bound metal in each cell was calculated from the relationship $(^{65}\text{Zn in retentate} - ^{65}\text{Zn in diffusate}) / (^{65}\text{Zn in retentate} + ^{65}\text{Zn in diffusate})$. We observed no change in the relative volumes of the protein and chelator compartments during dialysis. The final pH was measured at 22 °C with a Radiometer GK2302C ceramic junction combination electrode.

Metal-Ligand Equilibria and Calculations of Ionic Zn. Standard equilibrium equations and equations for computing the concentration of Zn^{2+} ion have been derived and are available on request.

Scatchard Analysis. Traditional Scatchard analysis plots the relationship between the ratio of protein-bound metal to

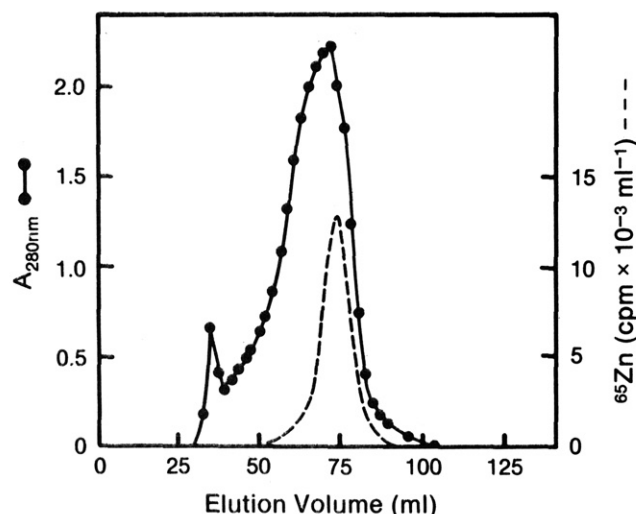


FIGURE 1: Typical elution profile of ^{65}Zn -labeled albacore blood plasma on Sepharose 6B-200 reduced. HEPES/NaCl buffer, pH 7.0.

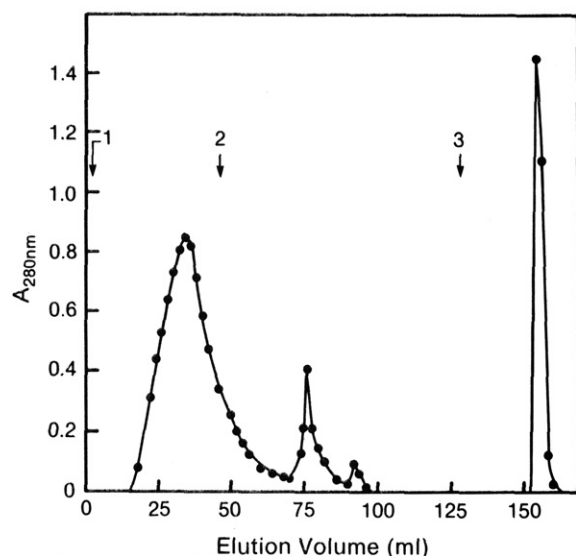


FIGURE 2: Typical elution profile of pooled radioactive peak from Sepharose 6B-200 (Figure 1) on chelating Sepharose 6B (Zn^{2+} form). Arrows: 1, sample loaded and column washed; 2, pH gradient begins; 3, column wash begins.

free metal vs. protein-bound metal. For this treatment, "free" metal is considered to be the difference between metal presented and metal bound to protein (Scatchard, 1949). Siiteri (1984) points out that, in binding studies, the appropriate value for the "free" component (in our case, zinc) is the active species which is not bound to any other moiety in the system. In our experiments, zinc has been presented to the protein in the form of its NTA chelate. This reduces the availability of the zinc for binding except to sites with an affinity greater than NTA. According to Siiteri's suggestion, the values used for "free" zinc in our Scatchard plots are those obtained by calculating ionic zinc (Zn^{2+}) only.

RESULTS

Protein Purification. Figures 1–3 show typical elution profiles for the sequential purification of the Zn protein from albacore plasma on Sepharose 6B, chelating Sepharose 6B, and concanavalin A-Sepharose 4B, respectively. Metal-binding protein peaks were identified by electrophoresis and by retention of ^{65}Zn . Table I shows the progress of purification attained at each chromatographic step. On the basis of "specific activity", a 7-fold enrichment for this protein was

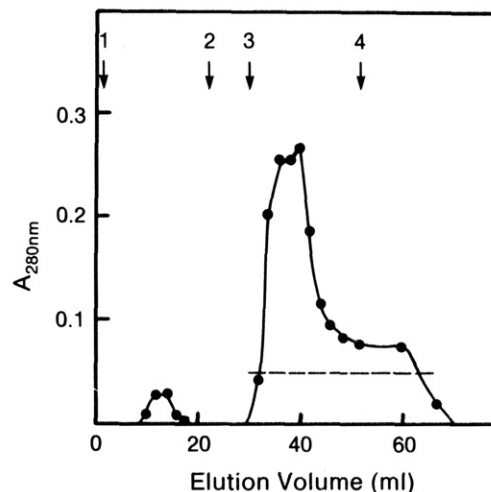


FIGURE 3: Typical elution profile of Zn peak from chelating Sepharose 6B (Figure 2) on concanavalin A-Sepharose 4B in phosphate/NaCl buffer, pH 7.0. Arrows: 1, sample loaded and column washed; 2, methyl mannoside loaded and equilibrated for 30 min with column; 3, column eluted with methyl mannoside; 4, column wash begins.

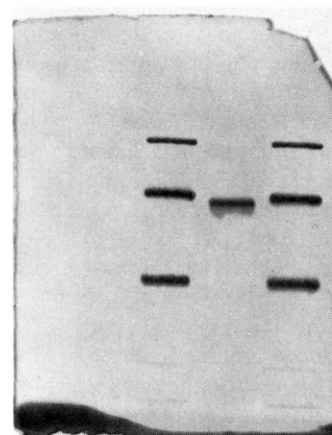


FIGURE 4: Acrylamide gel electrophoresis of Zn protein and comparison with molecular weight markers. Lanes 1 and 3 show phosphorylase b (M_r 92 500), bovine serum albumin (M_r 66 200), ovalbumin (M_r 45 000), carbonic anhydrase (M_r 31 000), and soybean trypsin inhibitor (M_r 21 500). Lane 2 shows the Zn protein estimated to be M_r 66 000.

Table I: Purification Table

method	total volume (mL)	total protein (mg)	zinc bound (μg)	zinc bound ($\mu\text{g}/\text{mg}$ of protein)
plasma	1	93.30	44.34	0.48
gel filtration	18	59.76	43.32	0.73
Zn affinity chromatography	5	13.30	22.02	1.66
lectin affinity chromatography	5	2.05	6.70	3.27

achieved over its original concentration in tuna plasma. Two milligrams of purified protein was recovered from 1 mL of plasma (Table I). This yield represents about 15% of the total Zn-binding capacity of plasma. We therefore estimate this protein to be 14% of the total plasma proteins, so that a 7-fold enrichment represents close to the maximum possible purification. The purity of the final protein peak was greater than 95% as judged by Kodavue staining after electrophoresis and integration of stainable bands (Figure 4) by scanning densitometry. We have made progress in sequencing approximately 30 N-terminal amino acids of the tuna plasma Zn-binding protein. It is more appropriate to present these data elsewhere in more complete form. However, only a single amino acid

Table II: Amino Acid Composition of Zinc-Binding Protein

amino acid	mol %	residues/mol ^a
Asp	10.64	62
Thr	5.15	30
Ser	6.33	37
Glu	9.36	55
Pro	3.13	18
Gly	7.56	44
Ala	7.06	41
Val	6.86	40
Met	2.99	17
Ile	4.43	26
Leu	6.72	39
Tyr	4.92	29
Phe	7.05	41
His	8.15	48
Lys	6.93	41
Arg	2.52	15
Cys ^b	0.20	1
Trp	nd ^c	
	100.00 ^d	584 ^d

^a Calculated by multiplying mole percent by 584 residues (66000 g/113 g per residue). ^b Cysteines were not protected. ^c nd = not determined. ^d Total.

signal has been observed at each degradation cycle. This result is strong evidence for homogeneity of this protein, since no contaminating N-terminal amino acids were detected. Molecular weight was estimated by the electrophoretic method of Weber and Osborn (1969) by reference to the R_f of molecular weight standards (Figure 4). The molecular weight of the Zn-binding protein was estimated to be 66 000.

Amino Acid Analysis. Table II shows the amino acid content of the Zn protein. Because cysteine was not protected, its value may be in error. The number of residues was calculated by dividing the average molecular weight of amino acids into the molecular weight of the protein. The value used as the average molecular weight per residue (113) was calculated by multiplying the mole percent contributed by each amino acid by its molecular weight, summing the products, and subtracting for the loss of one molecule of water. The total number of residues was then multiplied by the mole percent of each amino acid to give the number of residues per mole.

Stoichiometry Determined by Scatchard Plots. Primary data are given in Table III for binding experiments conducted in three pH ranges: 5.0, 7.0, and 8.5. Preliminary analysis of the binding data at pH 7.0 and 8.5 (Table III) confirmed the suggestion of Siiteri (1984) that the "free" (i.e., ionic and uncomplexed) zinc was the species involved in the metal-binding activity of this protein. For example, Scatchard plots of the ratio of moles of Zn:moles of protein (\bar{v}) vs. $\bar{v}/[\text{Zn}]$ were much more linear when the zinc term was Zn^{2+} rather than total zinc not bound to protein. Figures 5 and 6 show the Scatchard plots of pH 7.0 and 8.5 data presented in this way. Visual inspection of these plots suggests that the binding increased linearly with increasing Zn^{2+} concentration to a maximum, after which binding plateaued. For each pH experiment (7.0 and 8.5), we accordingly grouped data points into two classes by a process of maximizing the correlation coefficient for two independent data sets. The correlation coefficient for the data yielding line A at pH 7.0 is -0.892 ; that for the data yielding line B is 0.780 . The lines intersect at $\bar{v} = 3.26$. At pH 8.5, the correlation coefficient for line A is -0.971 ; that for line B is 0.581 . The lines intersect at $\bar{v} = 2.85$. Data from the pH 5.0 experiment did not fit a Scatchard plot because the slope of the line was positive. Notice the clustering of data points around $\bar{v} = 3$ where the "specific"

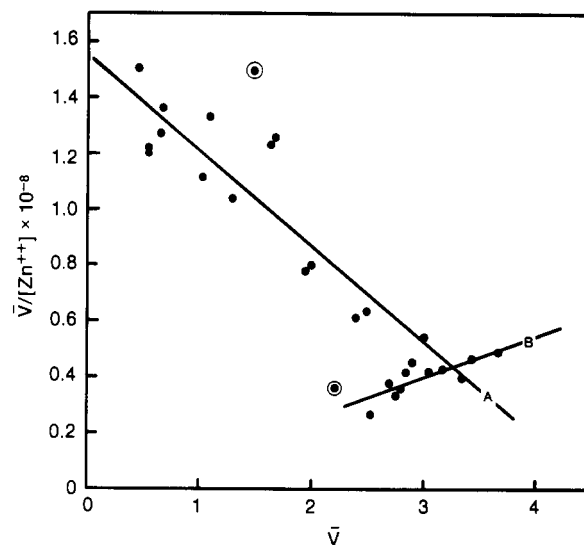


FIGURE 5: Scatchard plot of experimental data from equilibrium dialysis experiments at pH 7.0. Circled points (outliers) were eliminated from regression analysis.

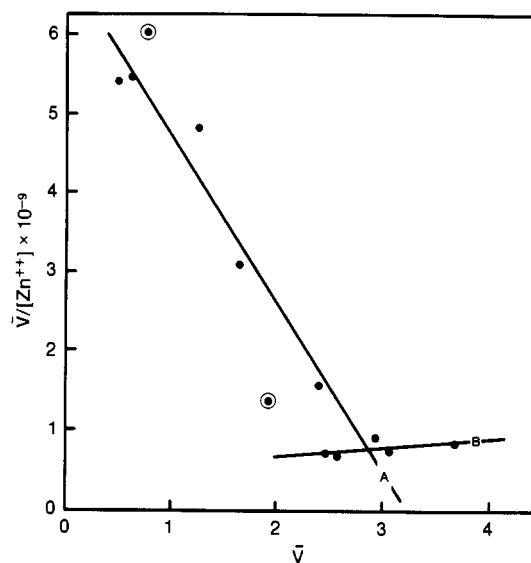


FIGURE 6: Scatchard plot of experimental data from equilibrium dialysis experiments at pH 8.5.

Zn-binding sites appear to be saturated. There are two reasons for the scatter of points around $\bar{v} = 3$. First, the protein has reached saturation, thereby preventing any real change in \bar{v} . Second, the experimental error increases at the higher zinc concentrations used. When zinc concentrations are low, the majority of the metal is found on the retentate side of the membrane, and the experimental error in subtracting a small number from a large number is small. However, at high zinc concentrations, the difference in zinc concentration between the two sides of the membrane is small, and the experimental error in subtracting two large numbers is correspondingly large. Therefore, the fluctuation in \bar{v} at saturation is more representative of the experimental error than of a real change in \bar{v} . Circled points (outliers) were eliminated from regression analysis because they fell outside the 95% confidence interval of the regression line. The data at pH 7.0 were also plotted (not shown) with \bar{v} vs. $[\text{Zn}]$, and show an asymptote at $\bar{v} \approx 3$. These data clearly show the protein binds 3 equiv of zinc.

Strength of Zinc Binding to Protein. Primary data for equilibrium dialysis experiments with Zn-binding protein are found in Table III. We were unable to calculate equilibrium constants for values of $\bar{v} \geq 3$, i.e., at saturation. When

Table III: Primary Data and Stoichiometric Equilibrium Constant for the Binding of Zinc to Albacore Serum Protein with NTA as the Competing Ligand

equilibrium concentration ($M \times 10^6$)				total zinc:protein ratio	$\bar{\nu}$	pH	-log free (ionic) zinc	log K^a	
NTA	total protein	protein- bound zinc	diffusible zinc					two histidines	three histidines
1.0320	1.5625	0.051	0.8865	0.6	0.0323	5.02	6.27	7.83	9.58
1.7203	1.5625	0.031	1.5320	1.0	0.0195	4.99	6.09	7.49	9.27
3.4406	1.5625	0.023	3.1020	2.0	0.0166	4.99	5.89	7.16	8.94
5.1609	1.5625	0.082	4.6060	3.0	0.0527	4.99	5.80	7.63	9.41
6.8812	1.5625	0.210	6.0400	4.0	0.1341	4.99	5.74	8.00	9.79
13.7625	1.5625	0.393	12.1070	8.0	0.2515	4.99	5.58	8.13	9.92
27.5250	1.5625	0.200	24.8000	16.0	0.1277	4.99	5.42	7.66	9.45
55.0500	1.5625	0.226	49.7740	32.0	0.1449	4.99	5.30	7.58	9.37
82.5750	1.5625	0.818	74.1820	48.0	0.5234	4.99	5.25	8.15	9.94
110.1000	1.5625	0.369	99.6310	64.0	0.2361	5.00	5.20	7.69	9.47
137.6250	1.5625	0.668	124.3320	80.0	0.4277	4.97	5.16	7.99	9.80
165.1500	1.5625	0.408	149.5920	96.0	0.2614	5.00	5.15	7.69	9.47
192.6750	1.5625	1.057	173.9430	112.0	0.6763	4.99	5.13	8.17	9.96
220.2000	1.5625	1.196	198.8040	128.0	0.7655	5.00	5.12	8.23	10.01
1.0320	1.5625	0.740	0.1975	0.6	0.4736	6.96	8.54	8.36	8.52
1.3762	1.5625	0.865	0.3850	0.8	0.5536	6.97	8.34	8.27	8.45
1.7203	1.5625	1.033	0.5300	1.0	0.6607	6.98	8.29	8.31	8.48
3.4401	1.5625	1.727	1.3980	2.0	1.1052	6.97	8.08	8.44	8.62
5.1609	1.5625	2.328	2.3600	3.0	1.4900	6.98	8.00	8.57	8.75
6.8812	1.5625	2.625	3.6250	4.0	1.6801	6.97	7.88	8.56	8.74
13.7625	1.5625	3.121	9.3790	8.0	1.9973	6.98	7.60	8.47	8.65
27.5250	1.5625	3.893	21.1070	16.0	2.4915	6.97	7.40	8.68	8.86
55.0500	1.5625	4.688	45.3120	32.0	3.0005	6.97	7.25		
82.5750	1.5625	4.439	70.5610	48.0	2.8409	6.99	7.17	8.98	9.15
110.1000	1.562	5.370	94.6300	64.0	3.4370	6.97	7.13		
137.6250	1.5625	4.319	120.6810	80.0	2.7640	6.98	7.08	8.72	8.89
165.1500	1.5625	5.224	144.7760	96.0	3.3432	6.97	7.07		
192.6750	1.5625	3.975	171.0250	112.0	2.5442	6.97	7.02	8.35	8.53
220.2000	1.5625	8.070	191.9300	128.0	5.1691	6.97	7.08		
1.0320	1.5625	0.721	0.2167	0.6	0.4613	6.98	8.51	8.34	8.52
1.3762	1.5625	0.863	0.3875	0.8	0.5520	6.98	8.34	8.27	8.44
1.7203	1.5625	1.050	0.5130	1.0	0.6720	6.98	8.31	8.34	8.51
3.4406	1.5625	1.627	1.4980	2.0	1.0413	6.98	8.05	8.34	8.52
5.1609	1.5625	2.027	2.6610	3.0	1.2973	6.98	7.91	8.36	8.53
6.8812	1.5625	2.577	3.6734	4.0	1.6491	6.98	7.87	8.53	8.70
13.7625	1.5625	3.049	9.4510	8.0	1.9511	6.99	7.60	8.43	8.60
27.5250	1.5625	3.715	27.2853	16.0	2.3774	6.99	7.40	8.55	8.72
55.0500	1.5625	3.455	46.5450	32.0	2.2113	7.00	7.21	8.21	8.37
82.5750	1.5625	4.540	70.4602	48.0	2.9055	7.01	7.20	9.22	9.38
110.1000	1.5625	4.233	95.7674	64.0	2.7089	7.02	7.15	8.64	8.79
137.6250	1.5625	4.761	120.2386	80.0	3.0473	7.03	7.14		
165.1500	1.5625	4.965	145.0350	96.0	3.1777	7.04	7.13		
192.6750	1.5625	4.383	170.6170	112.0	2.8049	7.04	7.10	8.76	8.90
220.2000	1.5625	5.735	194.2649	128.0	3.6700	7.05	7.12		
1.0320	1.5625	0.769	0.1685	0.6	0.4923	8.40	10.04	9.36	9.36
1.3762	1.5625	0.971	0.2790	0.8	0.6215	8.42	9.94	9.38	9.38
1.7203	1.5625	1.193	0.3700	1.0	0.7634	8.41	9.90	9.46	9.46
3.4406	1.5625	1.957	1.1680	2.0	1.2525	8.37	9.58	9.47	9.47
6.8812	1.5625	2.573	3.6770	4.0	1.6465	8.41	9.27	9.38	9.38
13.7625	1.5625	3.000	9.5000	8.0	1.9201	8.27	8.86	9.14	9.14
27.5250	1.5625	3.737	21.2630	16.0	2.3918	8.42	8.82	9.44	9.44
82.5750	1.5625	4.015	70.9850	48.0	2.5695	8.29	8.43	9.24	9.24
110.1000	1.5625	3.840	96.1600	64.0	2.4578	8.39	8.47	9.15	9.15
137.6250	1.5625	4.571	120.4290	80.0	2.9251	8.42	8.49	10.11	10.11
165.1500	1.5625	4.789	145.2110	96.0	3.0650	8.34	8.40		
192.6750	1.5625	5.775	169.2250	112.0	3.6959	8.29	8.36		
								8.96 ^b	9.39 ^b
								CV (%) 216.22 ^c	121.78 ^c

^aUnits = M^{-1} . ^bValues are expressed as the log of the mean of the " K ". ^cCV = coefficient of variation = the true standard deviation (not logarithmic) divided by the true mean multiplied by 100. Total zinc = protein-bound zinc + diffusible zinc. Due to the equilibrium formulation, when $\bar{\nu}$ is greater than 3, a constant could not be calculated.

Scatchard analysis is used to determine the number of binding sites on a macromolecule, the "binding constant" is often calculated from the slope of the line. However, with the additional information we have gained for this protein, we are able to determine a stoichiometric constant.

In order to calculate a stoichiometric equilibrium constant for the protein-metal interaction, several parameters must be

known: (1) the number of binding sites; (2) the nature of the binding sites (e.g., dependent, independent); (3) the amino acids involved in binding; and (4) the acid dissociation constants (pK 's) of those amino acids involved. Our Scatchard analysis reported above offers no evidence for more than one type of binding site. Thus, the three binding sites appear to be equivalent and independent. The sequence of the N-ter-

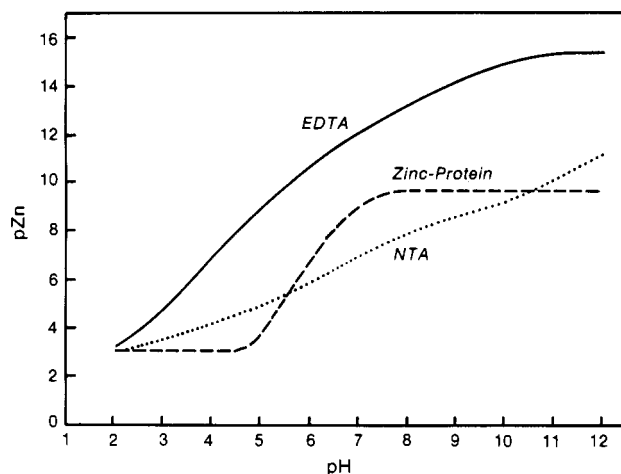


FIGURE 7: Free zinc ion concentration (expressed as $-\log [Zn^{2+}]$) computed as a function of pH in solutions of zinc and chelator (chelate:zinc ratio = 1:1:1). The zinc-ligand equilibria were solved for the following parameters: total zinc concentration, 1.0 mM; total ligand concentration (EDTA, NTA, or Zn protein), 1.1 mM; and association constant for the zinc-protein $[Zn(His)_3 \text{ protein}]$ complex, $10^{9.39} M^{-1}$.

minimal 30 amino acids of the protein shows a cluster of histidines and carboxylates, which we consider to be the most probable residues involved in binding. A full description of this work will be presented elsewhere. Two to four residues were used in our calculations, and every possible combination of the two types of amino acids at each pH was considered. Only two combinations listed in Table III (His_2 and His_3) yielded a reasonable fit with the experimental data. Only the inclusion of histidines affected the binding constant; the addition of carboxyl groups had an insignificant effect. Derivations of the apparent pK 's and equilibrium equations for calculating the stoichiometric binding constant have been calculated and are available upon request.

The mean of the computed stoichiometric equilibrium constants was $10^{8.96}$ for two histidines and $10^{9.39}$ for three histidines. The coefficient of variation of the data $[(SD/mean) \times 100]$ for three histidines involved in the binding was approximately half that for two histidines. The smaller relative coefficient of variation for the His_3 binding formulation indicates that this model gives a better fit with the data. Note that at pH 8.5 the log K values for two or three histidines are identical. At this pH, the histidines are fully deprotonated, and maximal binding is expected.

Strength of the Metal-Protein Chelate. The avidity of different chelators for a metal is best compared by displaying the concentration of uncomplexed (free) metal in the presence of excess chelator (Hegenauer et al., 1979). Because the association constant for the formation of a metal chelate is measured with respect to the fully dissociated ligand, uncomplexed metal will vary greatly depending upon pH. Therefore, it is inappropriate to judge the relative strength or affinity of metal binding solely by numerical comparison of association constants. However, we may display this competition between protons and metal by plotting free metal concentration as a function of pH. Figure 7 shows a comparison of pZn ($-\log [Zn^{2+}]$) computed at different pH values for zinc:chelator ratios of 1:1:1 for ethylenediaminetetraacetic acid (EDTA), NTA, and the albacore Zn protein. In this simulation, free zinc concentration in the presence of Zn protein reaches a minimum plateau beyond pH 8.0, where the histidines become fully dissociated. Between pH 5.7 and 10.5, the Zn protein is a better chelator than NTA and will accept zinc from the NTA chelate despite the fact that the numerical value of the

association constant of NTA for zinc is approximately 30 times greater than the association constant of the protein for zinc.

DISCUSSION

The binding of zinc to macromolecules in the serum of mammals has been studied extensively (Giroux & Henkin, 1972; Prasad & Oberleas, 1970; Parisi & Vallee, 1970; Evans & Hahn, 1974). The two major serum proteins responsible for binding zinc are albumin and α_2 -macroglobulin. Fletcher and Fletcher (1980) found an albumin-like Zn protein in the plasma of winter flounder which bound over 95% of the zinc in the plasma. We have identified and characterized a Zn protein in the plasma of albacore tuna which we believe to be similar to, if not identical with, that of the winter flounder. The albacore protein was the only protein in the plasma to show any significant zinc uptake. Our albacore protein is not albumin. It contains three times more histidine than human serum albumin (HSA) [16 residues for HSA (Henkin, 1974) and 48 for the albacore zinc protein (Table II)]. With a \bar{n} of 3, the albacore protein binds 3 times more zinc than HSA (Giroux & Henkin, 1972). The affinity of the albacore Zn protein is 100 times greater than HSA [Giroux & Henkin (1972); HSA = 10^7 ; albacore zinc protein = 10^9 ; Table III]. We believe the albacore Zn protein can now be considered a new zinc transport protein.

This protein was also found in skipjack and yellowfin tuna plasma (unpublished experiments). Preliminary equilibrium dialysis experiments using strongly denaturing conditions (6 M urea) showed no loss of binding activity, indicating the binding site to be structural rather than conformational. Further studies are under way to sequence the protein and elucidate the structure of the Zn site.

ACKNOWLEDGMENTS

We thank Dr. Hans K. Hegetschweiler for his assistance in programming and Matthew Williamson for the amino acid analysis.

Registry No. L-His, 71-00-1; Zn, 7440-66-6.

REFERENCES

- Aspberg, K., & Porath, J. (1970) *Acta Chem. Scand.* 24, 1839.
- Billo, E. J., Brito, K. K., & Wilkins, R. G. (1978) *Bioinorg. Chem.* 8, 461.
- Cohen, S. R., & Wilson, I. B. (1966) *Biochemistry* 5, 904.
- Evans, G. W., & Hahn, C. (1974) in *Trace Elements in Man and Animals* (Hoekstra, W. G., Suttie, J. W., & Ganther, H. E., Eds.) Vol. II, pp 497-499, University Park Press, Baltimore.
- Fletcher, P. E., & Fletcher, G. L. (1978) *Can. J. Zool.* 56, 114.
- Fletcher, P. E., & Fletcher, G. L. (1980) *Can. J. Zool.* 58, 609.
- Giroux, E. L., & Henkin, R. I. (1972) *Biochim. Biophys. Acta* 273, 64.
- Hegenauer, J. C., Tartof, K. D., & Nace, G. W. (1965) *Anal. Biochem.* 13, 6.
- Hegenauer, J., Saltman, P., & Nace, G. (1979) *Biochemistry* 18, 3865.
- Henkin, R. I. (1974) in *Protein-Metal Interactions* (Friedman, M., Ed.) pp 299-328, Plenum Press, London.
- Hrkal, Z., & Vodrazka, Z. (1977) *J. Chromatogr.* 135, 193.
- Lonnerdal, B., & Hoffman, B. (1981) *Biol. Trace Elem. Res.* 3, 301.
- Lowry, O. H., Rosebrough, N. J., Farr, A. L., & Randall, R. J. (1951) *J. Biol. Chem.* 193, 265.

- Malmstrom, B. G. (1953) *Arch. Biochem. Biophys.* 46, 345.
 Muszynska, G., Zhao, Y.-J., & Porath, J. (1986) *J. Inorg. Biochem.* 26, 127.
 Parisi, A. F., & Vallee, B. L. (1970) *Biochemistry* 9, 2421.
 Prasad, A. S., & Oberleas, D. (1970) *J. Lab. Clin. Med.* 76, 416.
 Scatchard, G. (1949) *Ann. N. Y. Acad. Sci.* 51, 660.
 Siiteri, P. K. (1984) *Science (Washington, D.C.)* 223, 191.
 Studier, F. W. (1973) *J. Mol. Biol.* 79, 237.
 Vallee, B. L. (1959) *Physiol. Rev.* 39, 443.
 Vinogradov, A. P. (1953) *The Elementary Chemical Composition of Marine Organisms* (English translation), p 523, Sears Foundation for Marine Research.
 Weber, K., & Osborn, O. (1969) *J. Biol. Chem.* 244, 4406.

Molecular Exchange at the Lipid-Rhodopsin Interface: Spin-Label Electron Spin Resonance Studies of Rhodopsin-Dimyristoylphosphatidylcholine Recombinants[†]

Nicholas J. P. Ryba,[†] László I. Horváth,^{‡§} Anthony Watts,^{||} and Derek Marsh^{*†}

Abteilung Spektroskopie, Max-Planck-Institut für biophysikalische Chemie, D-3400 Göttingen, Federal Republic of Germany, and Department of Biochemistry, University of Oxford, Oxford OX1 3QU, U.K.

Received November 4, 1986; Revised Manuscript Received January 16, 1987

ABSTRACT: The photoreceptor protein rhodopsin has been reconstituted with a single phospholipid species, dimyristoylphosphatidylcholine, at a range of different lipid/protein ratios, and the exchange rate at the lipid-protein interface has been determined from the electron spin resonance spectra of spin-labeled phosphatidylcholine. For recombinants with lipid/protein ratios in the range 41:1 to 102:1 (mol/mol), the electron spin resonance spectra of 1-acyl-2-[14-(4,4-dimethyloxazolidine-*N*-oxyl)stearoyl]-*sn*-glycero-3-phosphocholine consist of a fluid component similar to that found in pure lipid bilayers and a motionally restricted component corresponding to lipids whose motion is reduced by interaction with the intramembranous surface of rhodopsin. The relative proportion of the motionally restricted component increases with increasing protein content in the complex. Spectral subtraction with fluid and motionally restricted components (from fluid- and gel-phase lipid, respectively), which best fit the apparent components in the complex, reveals that 22 ± 2 lipids per 39 000-dalton protein are motionally restricted, independent of lipid/protein ratio and of temperature. Simulation of the two-component spectra with the exchanged-coupled Bloch equations gives values for both the fraction of motionally restricted component and the exchange rate between the two components. Using fixed motionally restricted and fluid component line shapes at a given temperature, it is possible to obtain a consistent description of the lipid/protein ratio dependence of the spectra at each temperature. The number of motionally restricted lipids obtained by simulation, allowing for exchange, is 23 ± 3 per 39 000-dalton protein, again independent of temperature and of lipid/protein ratio. The rate of lipid exchange off the protein is independent of lipid/protein ratio, as expected, and increases from $1.3 \times 10^7 \text{ s}^{-1}$ at 25 °C to $1.9 \times 10^7 \text{ s}^{-1}$ at 40 °C in the fluid phase of dimyristoylphosphatidylcholine.

The rod outer segment disc has an archetypal fluid membrane, most probably as a result of the preponderance of unsaturated chains in the membrane lipids. A high degree of mobility has been demonstrated for all its molecular components [see, e.g., Watts (1982)]. Rhodopsin, the principal protein in the membrane, has been found both to rotate rapidly (Cone, 1972) and to undergo fast translational motion (Poo & Cone, 1974) within the plane of the membrane. Both ESR¹ and NMR experiments (Watts et al., 1979, 1981; Pates et al., 1985; Brown et al., 1977; Zumbulyadis & O'Brien, 1979) have revealed rapid motions of the lipid component of the membranes, although qualitatively different spectral effects are observed because of the difference in characteristic time scale of the two spectroscopies (Bienvenue et al., 1982; Deese et al., 1981; Deese & Dratz, 1986).

A point of considerable interest is the coupling of the protein motions to those of the fluid lipids. This is necessary for a detailed description of the mechanism of the protein rotation

and translation and to describe the way in which the relatively rigid helical backbone of the protein is interfaced to its fluid lipid environment. For this aspect of the lipid/protein interaction, the exchange of lipids on and off the intramembranous surface of the protein is likely to play a decisive role.

Previously Davoust and Devaux (1982) have demonstrated that the distal ends of hydrocarbon chains covalently anchored to rhodopsin rapidly lift off the protein surface with a frequency of $\sim 10^7 \text{ s}^{-1}$. Davoust et al. (1983) have further demonstrated that, as expected, freely diffusible lipids approach the rhodopsin surface with a rate that is diffusion-controlled. In this work we take advantage of the two-component nature of the ESR spectra of spin-labeled lipids in lipid/protein systems [see e.g., Marsh and Watts (1982)] to estimate the exchange rate of freely diffusible lipids at the surface of rhodopsin. A consistent description is obtained of the dependence of the exchange rates on both temperature and lipid/protein ratio. The values of the measured exchange rates

[†] Dedicated to Prof. Albert Weller on the occasion of his 65th birthday.

[‡] Max-Planck-Institut für biophysikalische Chemie.

[§] Permanent address: Institute of Biophysics, Biological Research Centre, Szeged, Hungary.

^{||} University of Oxford. A.W. thanks EMBO for the award of a short-term fellowship.

¹ Abbreviations: DMPC, 1,2-dimyristoyl-*sn*-glycero-3-phosphocholine; 14-PCSL, 1-acyl-2-[14-(4,4-dimethyloxazolidine-*N*-oxyl)-stearoyl]-*sn*-glycero-3-phosphocholine; ROS, rod outer segment; OG, octyl glucoside (*n*-octyl β -D-glucopyranoside); ESR, electron spin resonance; Tris, tris(hydroxymethyl)aminomethane.